Article

Lipid Domain Morphologies in Phosphatidylcholine#Ceramide Monolayers

Mikko Karttunen, Mikko P. Haataja, Matti Sa#ily, Ilpo Vattulainen, and Juha M. Holopainen

Langmuir, **2009**, 25 (8), 4595-4600• DOI: 10.1021/la803377s • Publication Date (Web): 27 February 2009

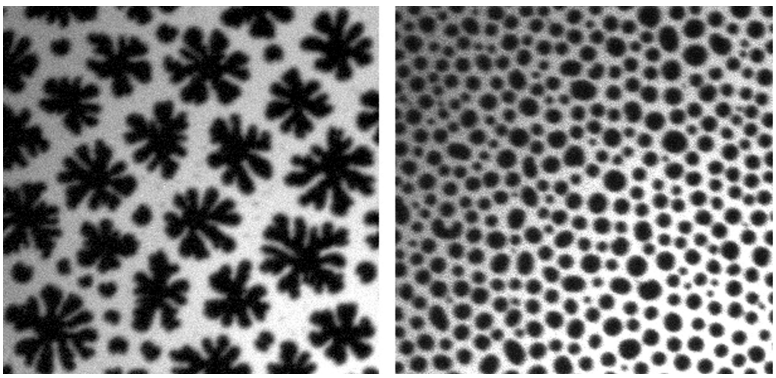

Langmuir
Article
pubs.acs.org/Langmuir

Lipid Domain Morphologies in Phosphatidylcholine−Ceramide Monolayers

Mikko Karttunen,[†] Mikko P. Haataja,[‡] Matti Säily,[§] Ilpo Vattulainen,[∥,⊥,#] and Juha M. Holopainen[▽,*]

[†]*Department of Applied Mathematics, the University of Western Ontario, London, Ontario, Canada,* [‡]*Department of Mechanical and Aerospace Engineering, Princeton Institute for the Science and Technology of Materials (PRISM), and Program in Applied and Computational Mathematics (PACM), Princeton University, Princeton, NJ,* [§]*Helsinki Biophysics & Biomembrane Group, Institute of Biomedicine, University of Helsinki, Finland,* [∥]*Department of Applied Physics, Helsinki University of Technology, Espoo, Finland,* [⊥]*Memphys−Center for Biomembrane Physics, University of Southern Denmark, Odense, Denmark,* [#]*Department of Physics, Tampere University of Technology, Tampere, Finland and* [▽]*Helsinki Eye Laboratory, Department of Ophthalmology, University of Helsinki, Finland*

Received October 12, 2008. Revised Manuscript Received February 1, 2009

In cells, one of the main roles of ceramide-enriched membrane domains is to recruit or exclude intracellular signaling molecules and receptors, thereby facilitating signal transduction cascades. Accordingly, in model membranes, even low contents of ceramide segregate into lateral domains. The impact of the *N*-acyl chain on this segregation and on the morphology of the domains remains to be explored. Using Langmuir monolayers, we have systematically studied binary mixtures of 1,2-dimyristoyl-*sn*-glycero-3-phosphocholine (DMPC) and ceramide (2:1, molar ratio) and varied the *N*-acyl chain length of ceramide from 2 to 24 carbon atoms (Cer_2 to Cer_{24}). Fluid Cer_2, Cer_6, and Cer_8/DMPC mixtures were miscible at all surface pressures. Longer ceramides, however, formed surface pressure-dependent immiscible mixtures with DMPC. The domain morphology under fluorescence microscopy after including a trace amount of fluorescent NBD-phosphatidylcholine into DMPC/Cer mixtures was found to be very sensitive to the *N*-acyl chain length. Shorter ceramides (Cer_{10}−Cer_{14}) formed flower-like (seaweed) domains, whereas longer ceramides (*N*-acyl chain length >14 carbon atoms) formed round and regular domains. We attribute the formation of the flower patterns to diffusive morphological instabilities during domain growth.

Introduction

Langmuir monolayers of amphiphiles, such as phospholipids, residing at the air/water interface show mesoscopic (i.e., micrometer scale) structure/domain formation in the course of a first-order phase transition between the isotropic and an anisotropic quasi-two-dimensional fluid phase.[1,2] Typically such monolayers are prepared in a Langmuir-type trough permitting a continuous decrease of the area per molecule (A), and resulting in an increase of the lateral pressure (π) along the film. Because the structures are mesoscopic, visualization of these coexisting phases can be made under Brewster angle microscopy or fluorescence microscopy after including a small amount of fluorescent probes into the monolayer.[3−5]

It has been almost universally thought that the equilibrium domain sizes as well as the shapes in lipid monolayers are determined by a competition between line tension and electrostatic dipolar repulsion of the charge-carrying headgroups.[1,2,6−9] In the same spirit, it has been proposed that properties such as chirality, hydrogen bonding capacity, and the spontaneous curvature of the constituent lipids might be *additionally* important in determining the shape of these domains.[10,11] While dipolar interactions are indeed important in many other systems, phase transformation kinetics may lead to metastable nonequilibrium domains, whose size and shape reflect the history of the phase transformation process. Here, we propose a mechanism based on such ideas. The present concept complements other principles that have been proposed for pattern formation over the past few years.[12−14]

As for membrane lipids, let us first highlight the importance of sphingolipids. They can be found in all eukaryotic cells: the major phosphosphingolipid sphingomyelin is very abundant in the outer leaflet of the plasma membrane constituting $\sim$ 30% of all lipids in that membrane.[15] The structure of sphingolipids is based on the long chain sphingosine, which is subsequently *N*-acylated to form ceramide; more complex sphingolipids are formed by the addition of polar headgroups to the C1 position of ceramide.[16] In cells, ceramide is formed by the hydrolysis of sphingomyelin by sphingomyelinase to yield ceramide and a water-soluble phosphocholine, or

*Corresponding author. Address: Helsinki Eye Laboratory, Department of Ophthalmology, University of Helsinki, Haartmaninkatu 4 C, 00290 Helsinki, Finland. Tel: +358 9 4717 7197; e-mail: juha.holopainen@hus.fi.

(1) Möhwald, H.. *Annu. Rev. Phys. Chem.* **1990**, *41*, 441–476.
(2) McConnell, H. M. *Annu. Rev. Phys. Chem.* **1991**, *42*, 171–195.
(3) Lösche, M.; Sackmann, E.; Möhwald, H. *Ber. Bunsenges. Phys. Chem.* **1983**, *87*, 848–852.
(4) Weis, R. M.; McConnell, H. M. *J. Phys. Chem.* **1985**, *89*, 4453–4459.
(5) Hénon, S.; Meunier, J. *Rev. Sci. Instrum.* **1991**, *62*, 936–939.
(6) Keller, D. J.; Korb, J. P.; McConnell, H. M. *J. Phys. Chem.* **1987**, *91*, 6417–6422.
(7) Vanderlick, T. K.; Möhwald, H. *J. Phys. Chem.* **1990**, *94*, 886–890.
(8) Seul, M.; Andelman, D. *Science* **1995**, *267*, 476–483.
(9) Ruckenstein, E. *J. Colloid Interface Sci.* **1997**, *196*, 313–315.
(10) Weis, R. M.; McConnell, H. M. *Nature (London)* **1984**, *310*, 47–49.
(11) Krüger, P.; Lösche, M. *Phys. Rev. E.* **2000**, *62*, 7031–7043.
(12) Bruinsma, R.; Rondelez, F.; Levine, A. *Eur. Phys. J. E* **2001**, *6*, 191–200.
(13) Flores, A.; Ize, P.; Ramos, S.; Castillo, R. *J. Chem. Phys.* **2003**, *119*, 5644–5653.
(14) Flores, A.; Corvera-Poiré, E.; Garza, C.; Castillo, R. *Europhys. Lett.* **2006**, *74*, 799–805.
(15) Rothman, J. E.; Lenard, J. *Science* **1977**, *195*, 743–753.
(16) Huwiler, A.; Kolter, T.; Pfeilschifter, J.; Sandhoff, K. *Biochim. Biophys. Acta* **2000**, *1485*, 63–99.

alternatively by *de novo* synthesis of ceramide.[17−19] Ceramide has been confirmed to function as a second messenger in several cellular processes, including apoptosis, growth suppression, differentiation, and cell senescence (for reviews, see, e.g., refs 17 and 18). Yet the downstream signaling events remain to be elucidated. Ceramides are very hydrophobic and reside at the place of its production,[20] thus ceramides generated in various organelles might show their activity at the site of production. In keeping with this, ceramide generated by the acidic sphingomyelinase in the lysosome remains in this organelle.[21]

Ceramide bilayers are highly ordered and show a high main phase transition temperature that is probably due to minimal hydration and strong hydrogen bonding capacity between ceramide headgroups.[22,23] In keeping with this, fully hydrated *N*-palmitoylsphingosine (Cer16) displays the main phase transition at 90−93 °C. Interestingly, this transition is independent of the *N*-acyl chain length of ceramides from 16 to 20 carbon atoms.[24,25] In Langmuir monolayers, Löfgren and Pascher[26] showed that *N*-octadecanoyl-sphingosine (Cer_{18}) and *N*-nervonoyl-sphingosine ($Cer_{24:1}$) revealed expanded to condensed force−area isotherms lacking any additional phase transitions between two mesomorphic states of the lipid monolayer. The small collapse area (~40 Å^2) measured for these lipids indicated that the hydrocarbon chains were packed into crystalline arrays with chains perpendicular to the air/water interface resembling the monolayer packing of long-chain fatty acids.

We and others[27,28] have studied mixtures of ceramides and phosphatidylcholines in Langmuir monolayers. We previously characterized the behavior of mixtures of Cer_{16} and $Cer_{24:1}$ with 1,2-dimyristoyl-*sn*-glycero-3-phosphocholine (DMPC). Cer_{16} was shown to be highly immiscible with DMPC, whereas the longer and unsaturated *N*-acyl chain was substantially more miscible into the DMPC matrix.[27] Importantly, the domain morphologies for the two ceramides mixed with DMPC were distinctively different. For the Cer_{16}/DMPC 1:1 mixture, dark ceramide-enriched domains exhibited a complex network with some round domains entrapped into the bright continuum. $Cer_{24:1}$/DMPC films exhibited already at low ceramide concentrations flower-like solid domains.

The current study was undertaken to systematically explore the effect of changing the length of the *N*-acyl chain of ceramide on domain morphology. Despite a number of studies, domain growth in Langmuir monolayers is not fully understood. Yet these systems display very rich and diverse phenomena. As a recent elegant example, Flores et al.[13,14] explained pattern formation in a single-component monolayer using stability concepts from dendritic growth and dynamic phase transitions, and Bruinsma et al.[12] have suggested a pattern formation mechanism based on the Marangoni instability. In this article, we argue that the different domain morphologies arise from a subtle interplay between nucleation and growth. Specifically, surface pressure acts as a driving force for the formation of the ceramide-rich gel phase, and these gel domains grow by excluding DMPC molecules. It is well-known since the seminal work by Mullins and Sekerka[29] that this type of growth typically results in the formation of morphological instabilities and flower-like patterns in the regime where nucleation rates are slow. At fixed surface pressure, however, an increase in the ceramide chain length increases the driving force for the phase transformation due to attractive van der Waals interactions.[1] Additionally, an increasing chain length of ceramide drives changes in ceramides' conformational and hydrogen bonding properties, which favor clustering at very low surface pressures.[30] Thus, nucleation is enhanced, and the domains saturate in size before diffusional instabilities take over. We will discuss this view in more detail below.

Materials and Methods

DMPC was obtained from Sigma (St. Louis, MO). Ceramides were from Avanti Polar Lipids, Inc. (Alabaster, AL), and NBD-PC was purchased from Molecular Probes (Eugene, OR). Their purity was checked by thin-layer chromatography on silicic acid-coated plates (Merck, Darmstadt, Germany) using chloroform/methanol/water (65:25:4, v/v/v) for DMPC and NBD-PC, and 1,2-dichloroethane/methanol/water (90:20:0.5, v/v/v) as the solvent system for the ceramides. Examination of the plates after iodine staining revealed no impurities. Concentrations of the lipids were determined gravimetrically using a high-precision electrobalance (Cahn, Cerritos, CA).

Compression Isotherms. A computer-controlled Langmuir-type film balance μThrougS (Kibron, Inc., Helsinki, Finland) was used to record compression isotherms ($\pi-A$). All glassware used was rinsed thoroughly with ethanol and purified water (Millipore). To ensure complete evaporation of the solvents, the films were allowed to settle for 10 min before recording the $\pi-A$ isotherms. Lipids (ceramide/DMPC 1:2 molar ratio) were dissolved in chloroform and spread in this solvent (1 mg/mL) onto the buffer (10 mM phosphate−saline buffer, 1 M NaCl, pH 6.6) at ~25 °C. The monolayers were compressed at a rate of 4 Å^2/molecule/min. Surface pressure π is defined as

$$\pi = \gamma_0 - \gamma$$

where γ_0 is the surface tension of the air/buffer interface, and γ is the value for surface tension in the presence of a lipid monolayer compressed at varying packing densities. Monolayer surface potential (ΔV) was measured using the vibrating plate method (μSpot, Kibron, Inc.). All compression isotherms were repeated at least two times to ensure reproducibility.

Fluorescence Microscopy of Monolayers. Lateral organization of the mixed monolayers of DMPC and ceramide was observed by fluorescence microscopy and using a computer controlled Wilhelmy-type film balance (μTrough S, Kibron,

(17) Hannun, Y. A. *J. Biol. Chem.* **1994**, *269*, 3125–3128.
(18) Hannun, Y. A. *Science* **1996**, *274*, 1855–1859.
(19) Jarvis, W. D.; Grant, S.; Kolesnick, R. N. *Clin. Cancer Res.* **1996**, *2*, 1–6.
(20) Venkataraman, K.; Futerman, A. H. *Trends Cell Biol.* **2000**, *10*, 408–412.
(21) Chatelut, M.; Leruth, M.; Harzer, K.; Dagan, A.; Marchesini, S.; Gatt, S.; Salvayre, R.; Courtoy, P.; Levade, T. *FEBS Lett.* **1998**, *426*, 102–106.
(22) Moore, D. J.; Rerek, M. E.; Mendelsohn, R.. *J. Phys. Chem. B* **1997**, *101*, 8933–8940.
(23) Li, L.; Tang, X.; Taylor, K. G.; DuPré, D. B.; Yappert, M. C. *Biophys. J.* **2002**, *82*, 2067–2080.
(24) Shah, J.; Atienza, J. M.; Duclos, R. I.Jr.; Rawlings, A. V.; Dong, Z.; Shipley, G. G. *J. Lipid Res.* **1995**, *36*, 1936–1944.
(25) Chen, H.; Mendelsohn, R.; Rerek, M. E.; Moore, D. J. *Biochim. Biophys. Acta* **2000**, *1468*, 293–303.
(26) Löfgren, H.; Pascher, I. *Chem. Phys. Lipids* **1977**, *20*, 273–284.
(27) Holopainen, J. M.; Brockman, H. L.; Brown, R. E.; Kinnunen, P. K. J. *Biophys. J.* **2001**, *80*, 765–775.
(28) Carrer, D. C.; Maggio, B. *J. Lipid Res.* **1999**, *40*, 1978–1989.
(29) Mullins, W. W.; Sekerka, J. J. *Appl. Phys.* **1963**, *34*, 323–329.
(30) Vaknin, D.; Kelley, M. S. *Biophys. J.* **2000**, *79*, 2616–2623.

Inc., Helsinki, Finland), as described earlier.[27] The trough was mounted on the stage of an inverted microscope (Zeiss IM-35, Jena, Germany), and the quartz-glass window in the bottom of the trough was positioned over an extra long working distance 20× objective (Nikon). A 450−490 nm bandpass filter was used for excitation, and a 520 nm long-pass filter was used for emission. Images were recorded with a Peltier-cooled 12-bit digital camera (C4742-95, Hamamatsu, Japan) operating with running image processing software (HiPic, version 4.2.0, Hamamatsu, Japan). NBD-PC ($X = 0.01$) was used as a fluorescent probe. Stock solutions of the probe and the lipids, DMPC/ceramide/NBD-PC at a molar ratio of 66:33:1, were prepared in chloroform (~1 mg/mL) and stored at −20 °C. These mixtures were applied on the air−buffer (10 mM phosphate−saline buffer, 1 M NaCl, pH 6.6) interface using a Hamilton microsyringe to initial areas of 100 ± 10 Å^2/acyl chain (for the sake of clarity we consider the sphingosine backbone of ceramide as an acyl chain). After an equilibration period of 10 min, the monolayers were compressed symmetrically using two barriers at a rate of 2.5 Å^2/acyl chain/min. After reaching the indicated values for surface pressure (π), the compression was stopped, and the monolayer was allowed to settle for 2−4 min prior to recording the image. All measurements were done at an ambient temperature of 25 ± 1 °C and were repeated at least twice.

Results

We have previously characterized mixed monolayers of Cer_{16}/DMPC and $Cer_{24:1}$/DMPC monolayers and found that the domain morphology of these mixtures was distinctively different.[27] Accordingly, here we systematically studied the effect of the *N*-acyl chain of ceramide on the domain morphology. We used a series of saturated synthetic *N*-acyl chain-sphingosines, i.e., ceramides. The *N*-acyl chain length was varied from 2 to 24 carbon atoms. We will concentrate on the results of Cer_{12}, Cer_{14}, Cer_{16}, and Cer_{18} mixtures with DMPC and only briefly discuss the other lipid mixtures. In all experiments, the molar ratio was kept constant at a ratio of 1:2 for ceramide/DMPC. Force−area isotherms were recorded, and these films were further investigated by fluorescence microscopy.[31] For Cer_2/DMPC film at high surface pressure, ceramide was partly solubilized, as evidenced by a small area/lipid at film collapse and by a considerably large hysteresis in decompression of the film (not shown). Likewise, it seemed that Cer_6/DMPC monolayers were somewhat unstable based on hysteresis on decompression. All other films were stable.

The fluorescent lipid analogue, NBD-PC (molar fraction $X = 0.01$) readily partitions into the liquid-expanded domains in the coexistence region.[4] At 25 °C and at all surface pressures below film collapse, neat DMPC monolayers were chain-disordered, i.e., liquid-expanded and showed a collapse pressure of approximately 48 mN/m. Fluorescence microscopy of these monolayers revealed homogeneous distribution of the probe regardless of π, consistent with the liquid-expanded behavior (data not shown). Likewise, no discernible phase transitions were observed for mixtures of DMPC with very short chain ceramides (Cer_2 and Cer_6), and also the results of fluorescence microscopy of these monolayers were consistent with homogeneous distribution of probes up to the collapse pressure.

For Cer_2/DMPC (and also Cer_6/DMPC) film at high surface pressure, ceramide was partly solubilized as evidenced by a small area/lipid at film collapse and by a considerably large hysteresis in decompression of the film (data not shown). While a discontinuity for Cer_8/DMPC film was observed at ~37 mN/m, fluorescence microscopy of this film did not reveal any inhomogeneity at $\pi \leq 40$ mN/m. A clearly discernible liquid-expanded to liquid-condensed phase transition (LE→LC) was observed at ~25 mN/m for Cer_{10}/DMPC mixture, accompanied by the formation of irregular (flower-like) dark domains (data not shown). On the basis of X-ray diffraction and differential scanning calorimetry[32] and as discussed previously,[27] these dark NBD-PC depleted domains represent a solid ceramide enriched phase.

Increasing the *N*-acyl chain length of ceramide to Cer_{12} further lowered the LE→LC phase transition pressure to ~12−14 mN/m (Figure 1A), and this transition was accompanied by the formation of flower-like solid domains (Figure 2). Increasing the surface pressure increased the LC phase coverage from 0 at 10 mN/m to ~60% at 40 mN/m. The flower-like domain morphology changed to smoother morphologies in the time course of >1 h, but remained irregular even after 24 h (not shown). The long time necessary to form the equilibrium shape indicates most likely a weak line tension of ceramide enriched domains, a low mobility of ceramide molecules, or both. For Cer_{14}/DMPC mixtures and for longer ceramide/DMPC mixtures, the LE→LC phase transition was no longer visible (Figure 1A). The absence of such a transition at 25 °C suggests that these ceramides have little or no miscibility in DMPC monolayers.[27] Fluorescence microscopy of Cer_{14}/DMPC mixtures revealed already at very low surface pressures (<1 mN/m) the formation of flower-like domains (Figure 2). Compression of this mixture qincreased the LC phase coverage from 15 ($\pi = 10$ mN/m) to 55% ($\pi = 40$ mN/m). The flower-like domains were metastable and slowly (>1 h) adopted more rounded, yet irregular shapes (not shown).

Further increase in the *N*-acyl chain length of ceramide to Cer_{16} unexpectedly changed the domain morphology from flower-like to round and bean-like shapes (Figure 2). This round shape of the domains was observed also for Cer_{18}, Cer_{20}, and Cer_{24}/DMPC mixtures (not shown), although the size of these domains decreased at all surface pressures with increasing *N*-acyl chain length. In keeping with previous observations,[33] the domains were slightly larger at higher surface pressures.

To quantitatively compare the apparent condensing and expanding effects of different ceramides in a DMPC monolayer, we determined the mean molecular areas at four different surface pressures, viz., 10, 20, 30, and 40 mN/m (Figure 3A). These isobars show that, for short *N*-acyl ceramides (Cer_2 to Cer_8), increasing the number of carbon atoms slightly increases the average area per molecule. Further increase in the *N*-acyl chain to Cer_{10} induces a sharp decrease in A, which remains practically unaltered up to Cer_{16}. Thereafter further increase in the length of the *N*-acyl chain increases A.

To further characterize the effects of ceramide on membrane properties, we also measured surface potential−area ($\Delta V - A$) isotherms for ceramide/DMPC films. However, for these uncharged lipid species, ΔV represents the macroscopic average of the membrane dipole potential as a function of A. Taking into account the phase separation evident in

(31) Weis, R. M. *Chem. Phys. Lipids* **1994**, *57*, 227–239.

(32) Holopainen, J. M.; Lemmich, J.; Richter, F.; Mouritsen, O. G.; Rapp, G.; Kinnunen, P. K. J. *Biophys. J.* **2000**, *78*, 2459–2469.

(33) Helm, C. A.; Möhwald, H. *J. Phys. Chem.* **1988**, *92*, 1262–1266.

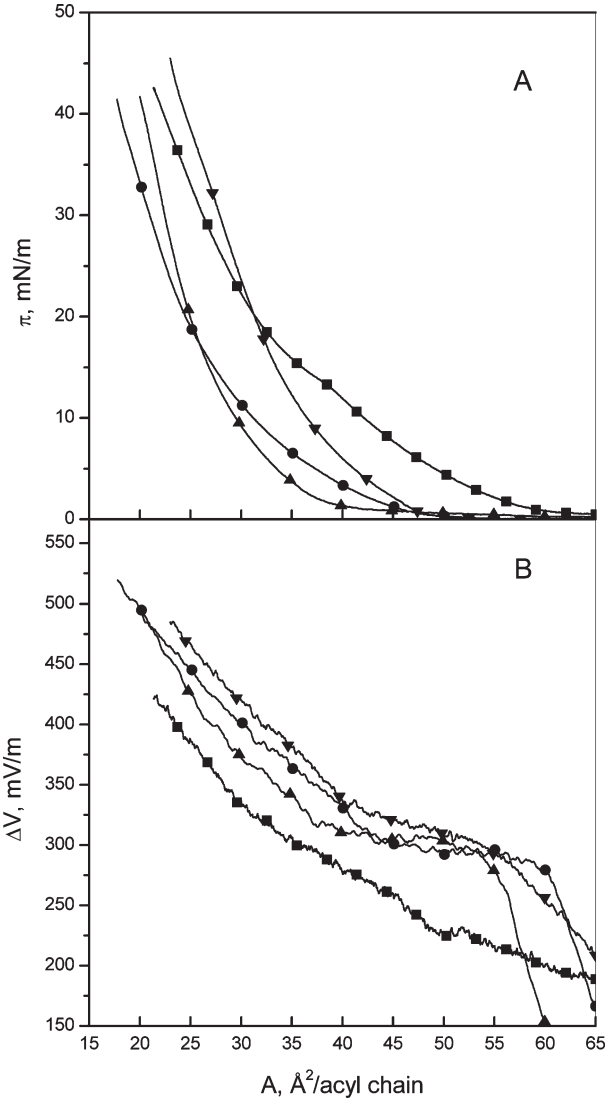

Figure 1. Panel A. Representative compression isotherms for Cer_{12}/DMPC (■), Cer_{14}/DMPC (●), Cer_{16}/DMPC (▲), and Cer_{18}/DMPC (▼) mixtures. Panel B. Representative surface potential V versus mean molecular area plots for Cer_{12}/DMPC (■), Cer_{14}/DMPC (●), Cer_{16}/DMPC (▲), and Cer_{18}/DMPC (▼) binary mixtures.

fluorescence microscopy images, the interpretation of the ΔV data is thus limited. Representative $\Delta V-A$ isotherms for Cer_{12}, Cer_{14}, Cer_{16}, and Cer_{18}/DMPC films are depicted in Figure 1B and show, as expected, that decreasing the area/molecule increases ΔV because compression causes the molecules to align in a more vertical orientation, thus affecting the vertical component of the measured potentials. To facilitate the viewing of $\Delta V-A$ isotherms, we have plotted the ΔV vs different ceramide isobars at four different surface pressures (π = 10, 20, 30, 40 mN/m) in Figure 3B. In essence, increasing the *N*-acyl chain length from 2 to 14 ceramide continuously increases ΔV, whereafter it remains practically unaltered. This may reflect the smaller size of the domains.

Discussion

The three-dimensional shape of cells has a great impact on their physiological state. For example, Chen et al.[34] showed that forcing the cells to grow on differently shaped microdishes determined whether individual cells grew or died. Thus, a yet unidentified machinery that recognizes the three-dimensional contour of a cell and possibly similar types of mechanism(s) may also identify two-dimensional platforms or "rafts" prevailing within cellular membranes. Cells contain a diverse set of chemically unique microdomains, which serve to concentrate signaling proteins and lipids and cellular receptors. Because of their characteristic chemical composition, it may be anticipated that the morphology of these domains varies, and this can in model membranes be achieved by simple modification of the lipid composition by enzymatic hydrolysis of the constituent lipids.[35] Khan et al.[36] recently showed that the cholesterol-binding protein NAP-22 identified raft-like lipid domains and, more importantly, the protein protected the lipid membrane from cholesterol extraction and simultaneously maintained the irregular morphology of the lipid domains. Accordingly, an intriguing possibility would be that cells could identify domains by their topography.

With short-chain ceramides (Cer_2−Cer_8), the substantial asymmetry of the *N*-acyl chain compared to the sphingosine base[37] allows the adjacent DMPC acyl chains to wobble more extensively, thus including these ceramides into DMPC has only a small effect on the average area per molecule (Figure 3A). Intermediate *N*-acyl chain length ceramides (Cer_{10}−Cer_{16}) are organized into ceramide-enriched gel-like domains, and the membrane becomes more condensed as aresult of a minimum in hydrophobic mismatch and increased van der Waals interactions. This is evident as a minimum in the average area per molecule (Figure 3A). These mixtures may behave like a uniform pseudocomplex mixture.[27] For asymmetric and long ceramides (*N*-acyl chain ≥16 carbon atoms), the end of the longer *N*-acyl chain protrudes above the monolayer. With these ceramides, a repulsive potential between ceramide molecules promotes miscibility with DMPC. This is evident in the larger average areas in A versus π isobars showing film expansion compared to shorter ceramides (Figure 3A). However, for longer ceramides, there should be an increased attractive potential due to van der Waals interaction between the protruding acyl chains. This is strengthened by the measured ΔV data (Figure 3B). Since it is the vertical component of the dipole moment that determines the measured potentials, ΔV increases monotonically as the length of the *N*-acyl chain is increased.

The domain shapes observed in this study are metastable and hence not in equilibrium; experimentally, it is practically impossible to observe thermodynamic equilibrium behavior in these systems over reasonable time scales. We can understand the emergence of distinct domain growth morphologies from the following simple physical picture. Long-chain ceramides start to nucleate as observable clusters already at very low surface pressures.[26,30] When nucleation is the driving force, the domains in a liquid are circular: there is no instability that becomes active under such conditions. Second, the domains, under any surface pressure, do not form hexagonal structures or lamellar domains, which would be typical equilibrium morphologies if dipolar interactions were the dominating factor.[1] For medium ceramide chain lengths at relatively low surface pressures, the growing domain is a (solid-like) gel phase, and domain growth proceeds by the *expulsion of DMPC* from the gel phase; the rate of growth of

(34) Chen, C. S.; Mrksich, M.; Huang, S.; Whitesides, G. M.; Ingber, D. E. *Science* **1997**, *276*, 1425–1428.

(35) Härtel, S.; Fanani, M. L.; Maggio, B. *Biophys. J.* **2005**, *88*, 287–304.

(36) Khan, T. K.; Yang, B.; Thompson, N. L.; Maekawa, S.; Epand, R. M.; Jacobson, K. *Biochemistry* **2003**, *42*, 4780–4786.

(37) Carrer, D. C.; Schreier, S.; Patrito, M.; Maggio, B. *Biophys. J.* **2006**, *90*, 2394–2403.

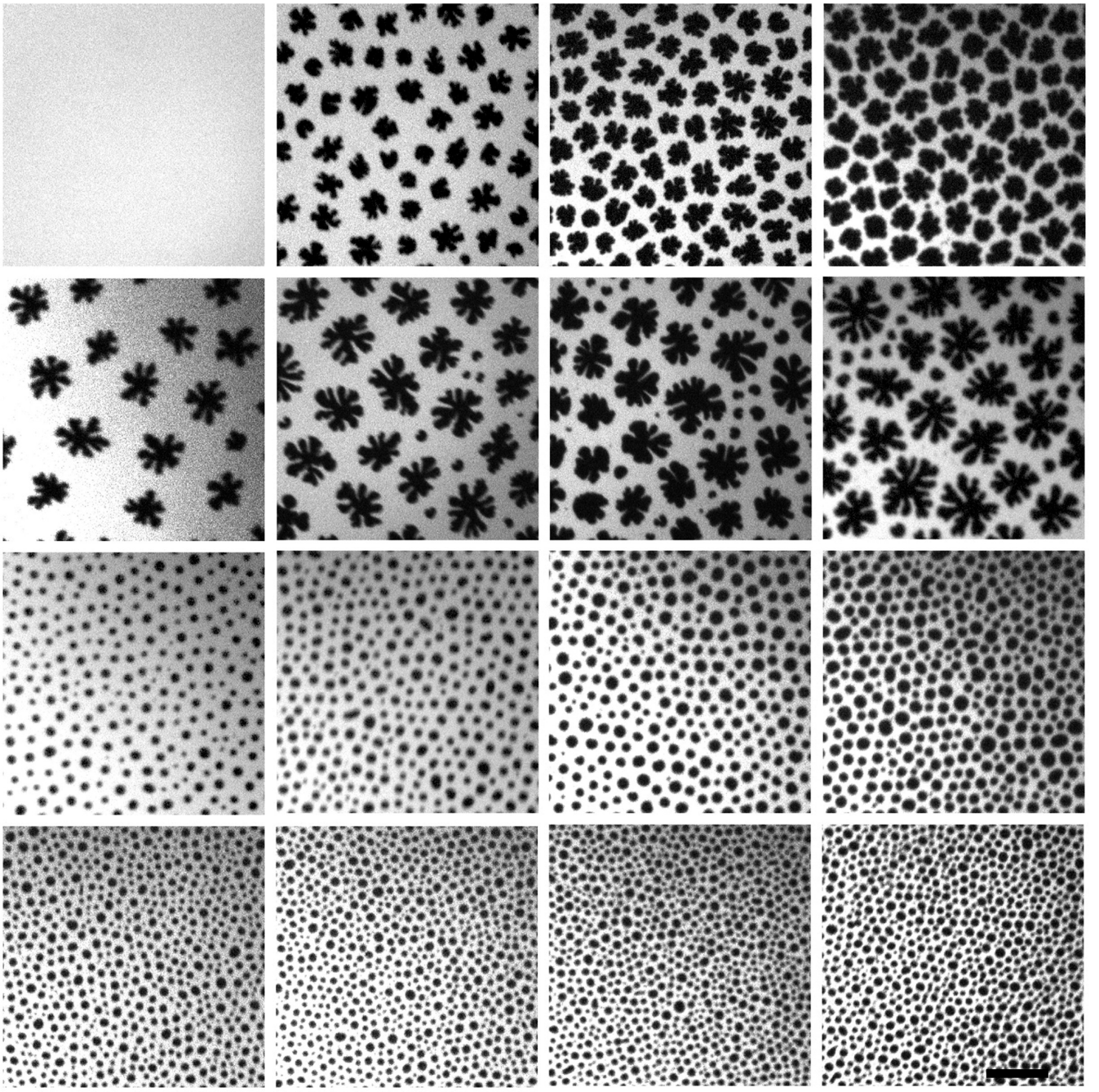

Figure 2. Fluorescence microscopy images of DMPC/ceramide/NBD-PC (66:33:1, molar ratio) monolayers at surface pressures (from left to right) of 10, 20, 30, and 40 mN/m. The first row represents representative images for Cer_{12}/DMPC, second row for Cer_{14}/DMPC, third row Cer_{16}/DMPC, and lowest row Cer_{18}/DMPC mixtures. Compression rate was 2.5 Å^2/acyl chain/min and the subphase was 10 mM phosphate-saline buffer, 1 M NaCl, pH 6.6. Images were recorded at 25 ± 1 °C. The scale bar represents 20 μm.

domains is limited by the diffusion of DMPC molecules away from the growth front: DMPC does not form a gel under the current experimental conditions.[38] Such diffusion-limited phase transformation processes are known to exhibit irregular growth morphologies, and the first quantitative explanation was put forth by Mullins and Sekerka,[29] who demonstrated that the growth front is morphologically unstable toward a small perturbation for a wide range of perturbation wavelengths. The most unstable wavelength sets the characteristic scale for the pattern, and it can be written[39]

$$\lambda_{MS} \sim (d_0 l_D)^{\frac{1}{2}}$$

where d_0 denotes the so-called capillary length (typically 1−10 nm) incorporating the gel−liquid line tension, and $l_D = 2D/v$ is the diffusion length; D is the diffusivity of DMPC, and v is the growth velocity. For $D = 10^{-11}$ m^2/s, $v = 10^{-6}$ m/s, and $d_0 = 10^{-9}$ m, one finds λ_{MS} to be $\sim 1.5 \times 10^{-7}$ m. In the case of an anisotropic capillary length, dendritic structures are observed,

(38) Nielsen, L. K.; Bjørnholm, T.; Mouritsen, O. G. *Langmuir* **2007**, *23*, 11684–11692.

(39) Langer, J. S. *Science* **1989**, *243*, 1150–1156.

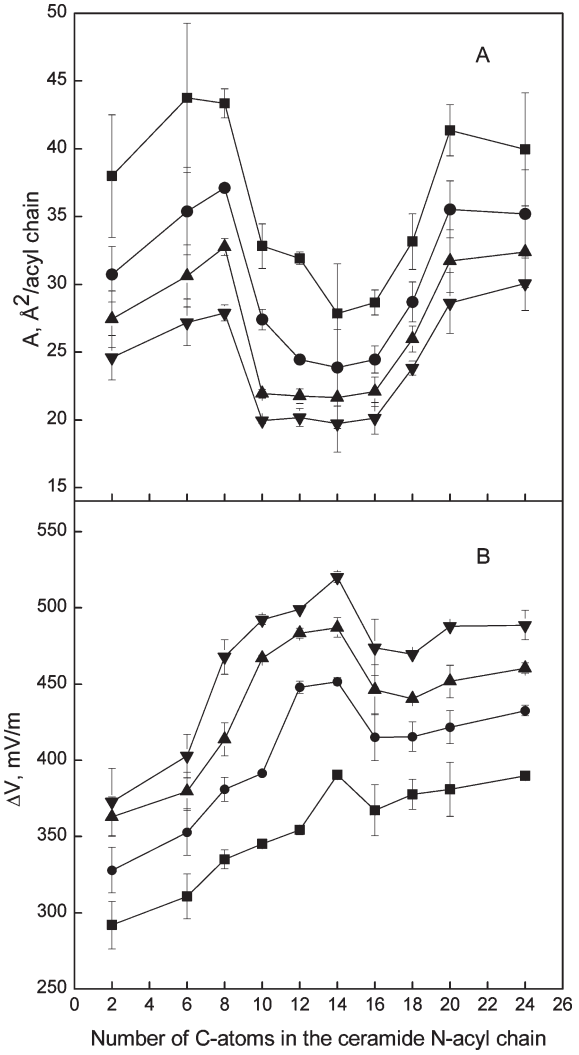

Figure 3. Mean molecular areas (panel A) and ΔV (panel B) vs the length of the *N*-acyl chain length for binary mixtures of ceramide and DMPC at 10 (■), 20 (●), 30 (▲), and 40 (▼) mN/m.

while, for an isotropic d_0, tip-splitting seaweed structures dominate.[40] For long ceramide chains, on the other hand, the driving force for the liquid−gel phase transition at fixed surface pressure is much larger because of the van der Waals interaction between the chains.[1] Thus, the morphology is governed by many small domains, which nucleate rapidly and do not grow large enough to display irregular growth morphologies. Specifically, rapid nucleation may suppress the formation of morphological instabilities by preventing the domains from reaching a critical size before they become unstable via the Mullins−Sekerka mechanism; the growth of the domains ceases once the phase transformation has run its course. Similarly, ideas based on instabilities and dynamic phase transitions have been used by Flores et al.[13,14] to explain pattern selection in single-component monolayers of dioctadecylamine, ethyl palmitate, and ethyl stearate. The seminal results based on dipole interactions[1,2,6−8] and current results by us, Flores et al.,[13,14] and Bruinsma et al.[12] suggest that there may be different mechanisms that drive pattern selection and morphologies depending on the nature of the system. All these results demonstrate the rich physics of monolayer systems and stress the fact that more systematic work is needed to understand the selection mechanisms.

One may argue that, since the domain morphology was not maintained for very long periods (on the order of hours) or that the observed domains are much larger than those in cells, these findings have no meaning in understanding cellular functions. On the contrary, we have to anticipate that cells are never in equilibrium, and their membranes are under continuous change in composition. The equilibrium size of phase-separated domains in model systems will be relatively large because the system minimizes energy associated with the phase boundaries. In fibroblasts, it was shown that the entire plasma membrane was changed within just 1 h.[41] In this regard, transient changes in the levels of Cer_{16} have been shown to be the trigger to induce apoptosis in Jurkat cells.[42] In this study, levels of other ceramide species remained unchanged. Our studies suggest that this effect may be due to instable formation of rigid ceramide domains, possibly with different thicknesses, that may either recruit certain downstream signaling proteins into well-defined and shaped domains, or may hamper the cellular signaling cascades, by disturbing protein and/or lipid distribution.

Acknowledgment. The authors thank professor Paavo Kinnunen for support during the preparation of the manuscript. M.K. would like to thank Prof. Ji-Ping Huang and the Department of Physics of Fudan University (Shanghai) for their warm hospitality. This work was supported by funding from the Sigrid Juselius Foundation (J.M.H.), the Academy of Finland (J.M.H., I.V.), the Finnish Cultural Foundation (J.M.H.), the Evald and Hilda Nissi Foundation (J.M.H.), The Finnish Eye Foundation (J.M.H.), and partly supported by an NSF-DMR Grant No. 0449184 (M.P.H.), and NSERC of Canada (M.K.).

Abbreviations

Cer_2	*N*-acetoyl-D-erythro-sphingosine
Cer_6	*N*-hexanoyl-D-erythro-sphingosine
Cer_8	*N*-octanoyl-D-erythro-sphingosine
Cer_{10}	*N*-decanoyl-D-erythro-sphingosine
Cer_{12}	*N*-lauroyl-D-erythro-sphingosine
Cer_{14}	*N*-myristoyl- D-erythro-sphingosine
Cer_{16}	*N*-palmitoyl- D-erythro-sphingosine
Cer_{18}	*N*-stearoyl-D-erythro-sphingosine
Cer_{20}	*N*-arachidoyl-D-erythro-sphingosine
Cer_{24}	*N*-lignoceroyl-D-erythro-sphingosine
$Cer_{24:1}$	*N*-nervonoyl-D-erythro-sphingosine
DMPC	1,2-dimyristoyl-*sn*-glycero-3-phosphocholine
LE→LC	liquid-expanded to liquid-condensed phase transition
NBD-PC	2-(12-(7-nitrobenz-2-oxa-1,3-diazol-4-yl)amino)dodecanoyl-1-hexadecanoyl-*sn*-glycero-3-phosphocholine
ΔV	surface potential
π	surface pressure

(40) Ihle, T.; Müller-Krumbhaar, H. *Phys. Rev. Lett.* **1993**, *70*, 3083–3086.

(41) Steinman, R. M.; Mellman, I. S.; Muller, W. A.; Cohn, Z. A. *J. Cell Biol.* **1983**, *96*, 1–27.

(42) Thomas, R. L.Jr; Matsko, C. M.; Lotze, M. T.; Amoscato, A. A. *J. Biol. Chem.* **1999**, *274*, 30580–30588.